

Dynamics of **Continuous, Discrete & Impulsive** **Systems**

Editor-in-Chief
Xinzhi Liu, University of Waterloo

Published as an added volume to DCDIS series B:
Applications and Algorithms, ISSN 1492-8760
2003

Watam Press · Waterloo

Numerical Analysis of Fast Charge Transport in Optically Sensitive Semiconductors

Roderick V.N. Melnik

University of Southern Denmark,
MCI, Faculty of Science and Engineering,
Sonderborg, DK-6400, Denmark
rmelnik@mci.sdu.dk

Janis Rimshans

Institute of Mathematics and Computer Science,
University of Latvia,
LV-1459, Riga, Latvia
rimshans@latnet.lv

Abstract— Novel applications in optoelectronics require the development of semiconductor structures with fast photo-response. Transport processes in such devices are dependent on quite complex, essentially nonlinear phenomena. In this paper we derive a model for the description of fast transient photo-response phenomena in GaAs-based transistors, and develop an unconditionally monotone conservative and absolutely stable numerical scheme for its solution. Numerical results are presented for GaAs vertical field-effect phototransistor structure. A major emphasis is given to photo-charge response in the depletion region of the structure.

I. INTRODUCTION

Photodevices with fast response are of a fundamental importance to optoelectronics and semiconductor industries. With a growing area of applications of such devices and a wider use of devices based on semi-insulating and relaxation semiconductor materials [11], a better understanding of carrier transport processes and subsequent optimisation of such devices represent an important task in theory and practice of semiconductor devices.

It is well known that many electro-optical properties of such devices (e.g., the resistance of electron gas) are very sensitive to optical illumination. In particular, illumination may reduce the number of electrons trapped on the “scattering centers” leading to enhancing electron gas mobility. With the development of new devices the role of such scattering centers can even be played by self-assembled quantum dots, if those are placed close enough to the electronic channel of a modulation doped field effect transistor (MODFET, e.g., [10]). Various ideas along this direction have been already studied in the literature and the development of novel applications of semiconductor structures with a narrow-gap “n” layer placed between two wide-gap barrier “N” layers is under way (e.g., [8] and references therein). In all these cases, studying transport of photoexcited electrons in these devices and the response of the photoconductive structure to fast optical pulses are of utmost importance. In addition, for a range of existing devices, such as HEBT (hetero-structure-emitter bipolar transistors) and VFEPT (vertical field-effect phototransistors), the illumination ef-

fect of semiconductor layers has many important applications [1, 2].

In this paper we have chosen a VFEPT structure as a case study example. The paper is organised as follows. In Section 2 we derive a drift-diffusion type model to describe the transient photo-response phenomena in GaAs-based VFEPTs. We are interested in describing fast processes that take place in the depletion region of the structure. In this case we show that a general model based on a system of five nonlinear partial differential equations can be simplified. In Section 3 we construct a numerical approximation for the system on a non-uniform grid and show, by using a consequence of the maximum principle, that the derived scheme is unconditionally monotone. This allows us to apply the scheme to the solution of convection dominated transport problems where the electrostatic field becomes large. In Section 4 we analyse the developed scheme numerically. Section 5 is devoted to computational results obtained with the developed scheme. Theoretical estimates on photo-response times to achieve steady state solutions are confirmed by numerical results obtained for different boundary conditions. Conclusions and future directions of the presented work are discussed in Section 6.

II. GOVERNING EQUATIONS

In what follows we are interested in the analysis of transport processes in semiconductor structures illuminated by the monochrome light. It is assumed that the structure is in the dynamic equilibrium in terms of concentration of conductive electrons, denoted further by n_c , and concentration of holes, denoted further by p_c . The photo-generated charge concentration are denoted further by n_e and p_e for electrons and holes, respectively. Then, electron-hole plasma of the semiconductor can be described by a coupled system of nonlinear equations containing continuity equations for each type of the carriers mentioned above and supplemented by the Poisson equation

$$\frac{\partial n_\alpha}{\partial t} - \frac{\partial J_n^\alpha}{\partial x} = -(R^\alpha - G^\alpha), \quad (1)$$

$$\frac{\partial p_\alpha}{\partial t} + \frac{\partial J_p^\alpha}{\partial x} = -(R^\alpha - G^\alpha), \quad (2)$$

$$\frac{\partial}{\partial x} \left(\kappa \frac{\partial \varphi}{\partial x} \right) = n_c - p_c + n_e - p_e - (N_d - N_a), \quad (3)$$

where densities of electron and hole currents (or carrier density fluxes) are defined by

$$J_n^\alpha = -\mu_n^\alpha n_\alpha \frac{\partial \varphi}{\partial x} + \frac{\partial}{\partial x} (\mu_n^\alpha n_\alpha T_n^\alpha), \quad (4)$$

$$J_p^\alpha = -\mu_p^\alpha p_\alpha \frac{\partial \varphi}{\partial x} - \frac{\partial}{\partial x} (\mu_p^\alpha p_\alpha T_p^\alpha). \quad (5)$$

In system (1)–(5) we use sub- or super-script α to denote both conductive and photo-generated carriers. In the context of the notation made this means that $\alpha = c$ for conductive carriers and $\alpha = e$ for photogenerated carriers. System (1)–(5) is given in normalised form, assuming DeMari's normalisation constants (e.g., [5] and references therein). Other notations used in (1)–(5) are standard. In particular, recall that R^α and G^α denote recombination and generation terms, respectively (note also that $G^c \equiv 0$), φ is the electrostatic potential (so that $-\frac{\partial \varphi}{\partial x}$ is the electrostatic field), μ and T (with corresponding sub/super-scripts) denote charge mobilities and temperatures, respectively, k is the dielectric constant of semiconductor material, and N_d and N_a are given concentrations of donor and acceptor impurities of the given structure. We consider a one-dimensional model and all experiments reported in Section 5 were obtained for a cross section of a VFEPT structure presented schematically in Fig. 1. Model (1)–(5) is considered in the

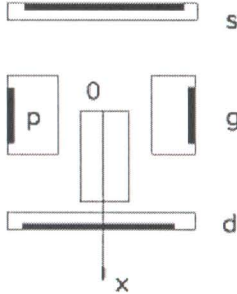


Fig. 1. Schematic representation of the structure under consideration

space-time region $\bar{\Gamma} = \{(x, t), 0 \leq x \leq L, 0 \leq t \leq T\}$. Boundary conditions for concentrations are assumed in the following general form

$$\eta \frac{\partial}{\partial x} n_\alpha(x, t) - \sigma n_\alpha(x, t) = a, \quad x = 0, \quad x = L, \quad (6)$$

incorporating Neumann, Dirichlet, and Robin boundary conditions by choosing appropriate coefficients η and σ , while for the potential, φ , we assume Dirichlet boundary conditions. Initial conditions for concentrations and potential were taken in the following form:

$$n_\alpha(x, 0) = n_0^\alpha(x), \quad p_\alpha(x, 0) = p_0^\alpha(x), \quad \varphi(x, 0) = \varphi_0(x). \quad (7)$$

By the (photo)response time of the device we understand the time needed to reach a steady-state photocurrent, and here we are interested in fast processes related to photoreponse phenomena. For example, such fast processes are in

the heart of phenomena in the depletion region of such devices as VFEPT. In this case, system (1)–(5) can be simplified by separating charge transport processes into fast and slow. Firstly, we re-write system (1)–(5) in an equivalent form, taking the sum and the difference of carrier concentrations as our new variables. In particular, consider the sum of equations (1) and (2) to get

$$\frac{\partial N_\alpha}{\partial t} - \frac{\partial}{\partial x} \delta F^\alpha = -2(R^\alpha - G^\alpha), \quad (8)$$

where $N_\alpha = n_\alpha + p_\alpha$ and $\delta F^\alpha = J_n^\alpha - J_p^\alpha$. It is easy to obtain that the flux difference δF^α is

$$\delta F^\alpha = -(\mu_n^\alpha n_\alpha - \mu_p^\alpha p_\alpha) \frac{\partial \varphi}{\partial x} - \frac{\partial}{\partial x} (\mu_n^\alpha n_\alpha T_n^\alpha + \mu_p^\alpha p_\alpha T_p^\alpha) + \frac{\partial}{\partial x} \{(\mu_n^\alpha T_n^\alpha + \mu_p^\alpha T_p^\alpha) N_\alpha\}. \quad (9)$$

In a similar way, from equations (1) and (2) we can also get

$$\frac{\partial \delta n_\alpha}{\partial t} - \frac{\partial}{\partial x} F^\alpha = 0, \quad (10)$$

where $\delta n_\alpha = n_\alpha - p_\alpha$ is the difference of charge concentrations, and $F^\alpha = J_n^\alpha + J_p^\alpha$ is the sum of carrier fluxes:

$$F^\alpha = -(\mu_n^\alpha n_\alpha + \mu_p^\alpha p_\alpha) \frac{\partial \varphi}{\partial x} + \mu_n^\alpha T_n^\alpha \frac{\partial p_\alpha}{\partial x} - \mu_p^\alpha T_p^\alpha \frac{\partial n_\alpha}{\partial x} + \frac{\partial}{\partial x} (\mu_n^\alpha T_n^\alpha) n_\alpha - \frac{\partial}{\partial x} (\mu_p^\alpha T_p^\alpha) p_\alpha + (\mu_n^\alpha T_n^\alpha + \mu_p^\alpha T_p^\alpha) \frac{\partial}{\partial x} \delta n_\alpha. \quad (11)$$

Having found N_α and δn_α , the actual concentrations can be easily reconstructed by using relations $n_\alpha = \frac{1}{2}(N_\alpha + \delta n_\alpha)$ and $p_\alpha = \frac{1}{2}(N_\alpha - \delta n_\alpha)$. In its generality, estimation of recombination at high excess charge concentrations is a difficult problem which can be addressed with transient photoconductivity measurements obtained as a function of the excitation density [4]. However, it is straightforward to notice that equations (10), (11) do not contain generation-recombination terms. Moreover, a simple analysis of fluxes (9) and (11) reveals that the drift contribution to (11) is much larger compared to the drift contribution to (9). Hence, in sufficiently high electric fields with high mobilities of carriers, it is equations (10), (11) that are responsible for fast processes. This equations will be in the main focus of our further consideration. Two remarks are left to conclude this section. Firstly, we note that in the present study we do not consider highly doped semiconductors and hence such effects as band gap narrowing are outside of the scope of the present paper. Secondly, to proceed with the solution of (10), (11) we still need an approximation to the spatio-temporal distribution of N_α . We assume that this distribution is practically unaffected by diffusion and recombination processes during the fast charge transfer stage in which we are interested in. In this case it is reasonable to assume that

$$N_\alpha = N_\alpha^0 + \delta n_\alpha, \quad (12)$$

where N_α^0 stands for the initial state value of this concentration.

III. CONSTRUCTING UNCONDITIONALLY MONOTONE NUMERICAL APPROXIMATIONS

The description of transient charge transport processes in semiconductor structures requires the development of numerical approximations that can be applied to both diffusion dominated cases and convection (drift) dominated cases. Due to a nonlinear character of these processes, monotone schemes without restrictions on step discretisations, known as unconditionally monotone schemes, would be ideally suitable for this task.

We introduce in the region $\bar{\Gamma}$, defined before, a nonuniform grid $\omega_{\tau h} = \omega_\tau \times \omega_h$, where $\omega_\tau = \{\tau_{l+1} = (t_{l+1} - t_l), l = 0, \dots, M_t - 1\}$, $\omega_h = \{h_{i+1} = (x_{i+1} - x_i), i = 0, \dots, M_x - 1\}$. The first step is standard and is carried out according to the integro-interpolational approach [9, 6]

$$\frac{(\delta n_\alpha)_{i+1}^{l+1} - (\delta n_\alpha)_i^l}{\tau_{l+1}} - \frac{(F^\alpha)_{i+1/2}^{l+1} - (F^\alpha)_{i-1/2}^{l+1}}{h_i^*} = 0, \quad (13)$$

where $1 \leq i \leq M_x - 1$, $0 \leq l \leq M_t - 1$, $(F^\alpha)_{i+1/2}$ is the averaged grid fluxes, and $h_i^* = \frac{1}{2}(h_{i+1} + h_i)$.

In order to obtain the averaged values of the grid fluxes $(F^\alpha)_{i+1/2}$, we introduce the exponential substitution for δn_α according to the following rule:

$$\delta n_\alpha = \Omega_n^\alpha(x, t) \exp(I_o^\alpha(x_0, x)), \quad (14)$$

where

$$I_o^\alpha(x_b, x_f) = \int_{x_b}^{x_f} dx \omega^\alpha(x), \quad (15)$$

and

$$\begin{aligned} \omega^\alpha(x) = & \frac{1}{\delta n_\alpha (\mu_n^\alpha T_n^\alpha + \mu_p^\alpha T_p^\alpha)} \\ & \left((\mu_n^\alpha n_\alpha + \mu_p^\alpha p_\alpha) \frac{\partial \varphi}{\partial x} - \mu_n^\alpha T_n^\alpha \frac{\partial p_\alpha}{\partial x} + \mu_p^\alpha T_p^\alpha \frac{\partial n_\alpha}{\partial x} \right. \\ & \left. - n_\alpha \frac{\partial}{\partial x} \mu_n^\alpha T_n^\alpha + p_\alpha \frac{\partial}{\partial x} \mu_p^\alpha T_p^\alpha \right), \end{aligned} \quad (16)$$

where x_0 is an arbitrary real number, not affecting the final form of the averaged flux representations, and $0 \leq x_b < x_f \leq L$. As a result of applying a procedure similar to that described in [5], we arrive to the following representation of the grid flux $(F^\alpha)_{i+1/2}$:

$$\begin{aligned} (F^\alpha)_{i+1/2} = & (\mu_n^\alpha T_n^\alpha + \mu_p^\alpha T_p^\alpha)_{i+1/2} (\beta_n^\alpha)_{i+1/2} \\ & \frac{(\delta n_\alpha)_{i+1} - \exp((\beta_n^\alpha)_{i+1/2}) (\delta n_\alpha)_i}{h_{i+1} (\exp((\beta_n^\alpha)_{i+1/2}) - 1)}, \end{aligned} \quad (17)$$

where

$$\begin{aligned} (\beta_n^\alpha)_{i+1/2} = & \frac{1}{(\mu_n^\alpha T_n^\alpha + \mu_p^\alpha T_p^\alpha)_{i+1/2} (\delta n_\alpha)_{i+1/2}} \\ & \left((\mu_n^\alpha n_\alpha + \mu_p^\alpha p_\alpha)_{i+1/2} (\varphi_{i+1} - \varphi_i) - \right. \\ & (\mu_n^\alpha T_n^\alpha)_{i+1/2} ((p_\alpha)_{i+1} - (p_\alpha)_i) + \\ & (\mu_p^\alpha T_p^\alpha)_{i+1/2} ((n_\alpha)_{i+1} - (n_\alpha)_i) - \\ & (n_\alpha)_{i+1/2} ((\mu_n^\alpha T_n^\alpha)_{i+1} - (\mu_n^\alpha T_n^\alpha)_i) + \\ & \left. (p_\alpha)_{i+1/2} ((\mu_p^\alpha T_p^\alpha)_{i+1} - (\mu_p^\alpha T_p^\alpha)_i) \right). \end{aligned} \quad (18)$$

Each value “a” at $x_{i+1/2}$ (that is $(a)_{i+1/2}$) in (18) is an approximation defined as $(a)_{i+1/2} = \frac{1}{2}((a)_{i+1} + (a)_i)$.

After substituting of $(F^\alpha)_{i+1/2}$ and $(F^\alpha)_{i-1/2}$ in the balance equation (13) we obtain the following numerical approximation for equation (10)

$$\begin{aligned} (\Lambda (\beta_n^\alpha) \delta n_\alpha^{l+1})_i \equiv & \frac{1}{h_i^*} A_i^{f\alpha} (\delta n_\alpha)_{i-1}^{l+1} + \\ & \frac{1}{h_i^*} B_i^{f\alpha} (\delta n_\alpha)_{i+1}^{l+1} - Q_i^{f\alpha} (\delta n_\alpha)_i^{l+1} = -\frac{(\delta n_\alpha)_i^l}{\tau_{l+1}}, \end{aligned} \quad (19)$$

where

$$Q_i^{f\alpha} = \frac{1}{h_i^*} (A_{i+1}^{f\alpha} + B_{i-1}^{f\alpha}) + \frac{1}{\tau_{l+1}}, \quad (20)$$

$$\begin{aligned} A_i^{f\alpha} = & (\mu_n T_n^\alpha + \mu_p T_p^\alpha)_{i-1/2} (\beta_n^\alpha)_{i-1/2} \\ & \frac{\exp((\beta_n^\alpha)_{i-1/2})}{h_i (\exp((\beta_n^\alpha)_{i-1/2}) - 1)}, \end{aligned} \quad (21)$$

$$\begin{aligned} B_i^{f\alpha} = & (\mu_n T_n^\alpha + \mu_p T_p^\alpha)_{i+1/2} (\beta_n^\alpha)_{i+1/2} \\ & \frac{1}{h_{i+1} (\exp((\beta_n^\alpha)_{i+1/2}) - 1)}. \end{aligned} \quad (22)$$

The derived scheme (19)–(22) is unconditionally monotone which can be easily verified by applying the maximum principle to the discrete problem. Conditions for the maximum principle in the case similar to ours (the one that contain first derivatives) have been first derived in [3]. By applying those conditions

$$\begin{aligned} (\Lambda (\beta_n^\alpha) \delta n_\alpha)_i \leq 0, \quad A_i^{f\alpha} > 0, \quad B_i^{f\alpha} > 0, \\ Q_i^{f\alpha} = \frac{1}{h_i^*} (A_{i+1}^{f\alpha} + B_{i-1}^{f\alpha}) + D, \quad D = \frac{1}{\tau_{l+1}} \geq 0 \end{aligned} \quad (23)$$

we confirm unconditional monotonicity of the derived scheme.

Spatio-temporal distribution of concentrations

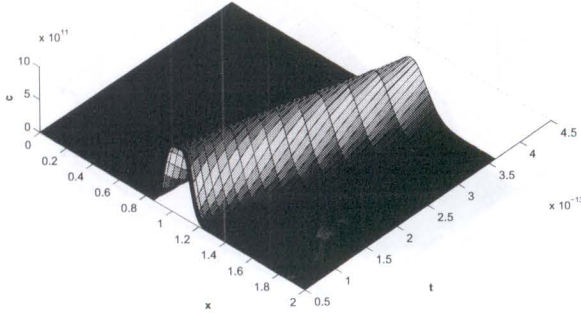


Fig. 2. Drift evolution in the VFEPT structure

Spatio-temporal distribution of potential energy

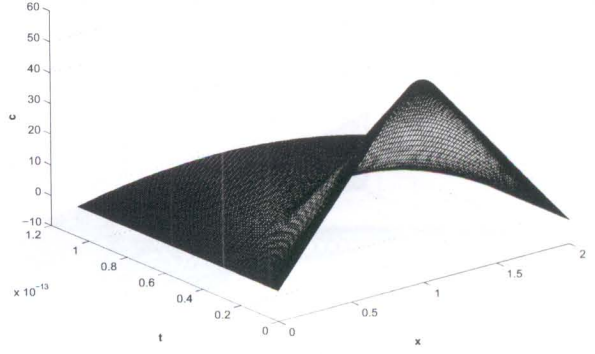


Fig. 4. Potential energy evolution

Spatio-temporal distribution of concentrations

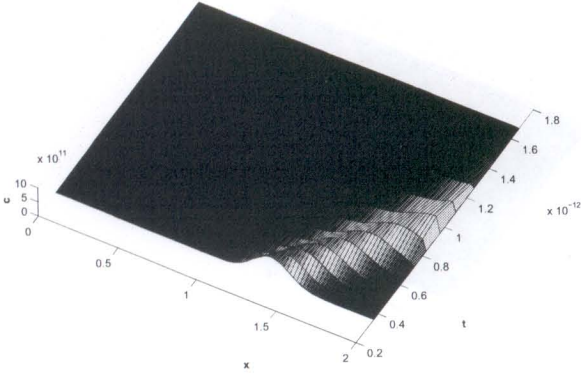


Fig. 3. Drift evolution in the VFEPT structure (estimating the drift time)

Spatio-temporal distribution of potential energy

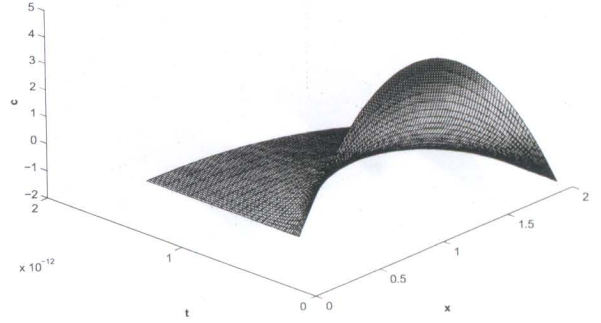


Fig. 5. Potential energy evolution

IV. ERROR ANALYSIS OF THE NUMERICAL APPROXIMATION

Whether the discretised model deals with a diffusion dominated or a convection dominated case can be judged upon by analysing coefficient β_n^α (see (18)). Indeed, the case where $\|(\beta_n^\alpha)\| \rightarrow 0$ corresponds to the diffusion dominated situation. This case can be considered in a way analogous to that proposed in [9] to show that the scheme considered here has the truncation error of second order. Our emphasis here, however, is on the case where $\|(\beta_n^\alpha)\| \rightarrow \infty$. We use perturbation arguments to show that in this limiting case the resulting scheme has the first order truncation error. First, we consider a perturbed value of β_n^α obtained from (18) by replacing n_α with $n_\alpha + 2\Delta$ and p_α by $p_\alpha + \Delta$, respectively, where Δ is an arbitrary chosen positive large constant such that $\Delta \gg N_\alpha, \Delta \gg \|\delta n_\alpha\|$. This value is denoted by $(\beta_n^\alpha)^*$ and

$$(\beta_n^\alpha)_{i+1/2}^* = \frac{1}{(\mu_n^\alpha T_n^\alpha + \mu_p^\alpha T_p^\alpha)_{i+1/2} ((\delta n_\alpha)_{i+1/2} + \Delta)}$$

$$((\mu_n^\alpha (n_\alpha + 2\Delta) + \mu_p^\alpha (p_\alpha + \Delta))_{i+1/2} (\varphi_{i+1} - \varphi_i) -$$

$$(\mu_n^\alpha T_n^\alpha)_{i+1/2} ((p_\alpha)_{i+1} - (p_\alpha)_i) +$$

$$(\mu_p^\alpha T_p^\alpha)_{i+1/2} ((n_\alpha)_{i+1} - (n_\alpha)_i) -$$

$$((n_\alpha)_{i+1/2} + 2\Delta) ((\mu_n^\alpha T_n^\alpha)_{i+1} - (\mu_n^\alpha T_n^\alpha)_i) +$$

$$((p_\alpha)_{i+1/2} + \Delta) ((\mu_p^\alpha T_p^\alpha)_{i+1} - (\mu_p^\alpha T_p^\alpha)_i)). \quad (24)$$

Secondly, we expand $\mu_n^\alpha, T_n^\alpha, \mu_p^\alpha, T_p^\alpha, \delta n_\alpha, N_\alpha$, and φ in the vicinity of the grid point with index i . The result, obtained by computer algebra tools of Mathematica, was substituted in (20)–(22) which allowed us to determine coefficients of the difference scheme under consideration. Then, the truncation error of the scheme can be evaluated by using the following representation:

$$\frac{\partial \delta n_\alpha}{\partial t} = \left(\frac{(\delta n_\alpha)^2}{(\delta n_\alpha + \Delta)^2} \right) \frac{\partial}{\partial x} F_d^\alpha +$$

$$\left(\frac{\Delta^2}{(\delta n_\alpha + \Delta)^2} \right) \frac{\partial}{\partial x} F_{dr}^\alpha + \mathcal{O} \left(\frac{\Delta}{(\delta + \Delta)^2} \right) +$$

Spatio-temporal distribution of excess carrier concentrations

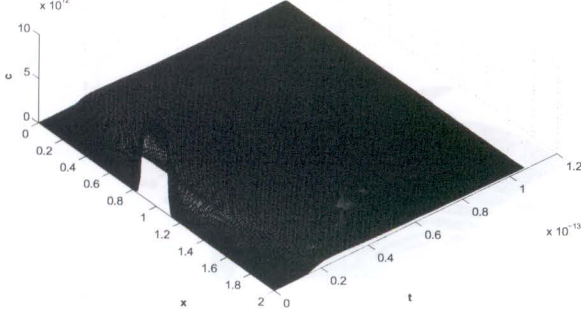


Fig. 6. Relaxation processes in the VFEPT structure (Dirichlet-Neumann boundary conditions)

Spatio-temporal distribution of excess carrier concentrations

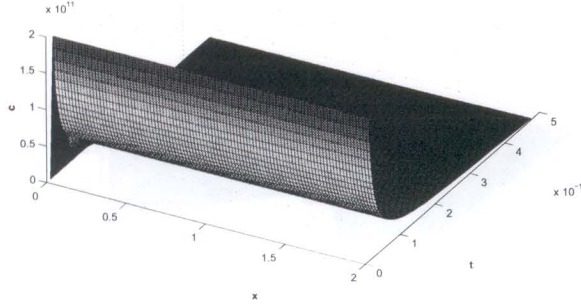


Fig. 7. Relaxation processes in the VFEPT structure (estimating relaxation time)

$$\mathcal{O}\left(\frac{1}{(\delta + \Delta)^2}h\right) + \mathcal{O}\left(\frac{\Delta^2}{(\delta + \Delta)^2}h\right), \quad (25)$$

where $\delta = \min(\delta n_\alpha)$. It is worthwhile noting that both terms, F_d^α and F_{dr}^α , represent drift dominated fluxes. Indeed, F_d^α given by the following expression

$$\begin{aligned} F_d^\alpha = & -(\mu_n^\alpha n_\alpha + \mu_p^\alpha p_\alpha) \frac{\partial \varphi}{\partial x} + \\ & \mu_n^\alpha T_n^\alpha \frac{\partial p_\alpha}{\partial x} - \mu_p^\alpha T_p^\alpha \frac{\partial n_\alpha}{\partial x} + \\ & \frac{\partial}{\partial x} (\mu_n^\alpha T_n^\alpha) n_\alpha - \frac{\partial}{\partial x} (\mu_p^\alpha T_p^\alpha) p_\alpha, \end{aligned} \quad (26)$$

can be obtained from (11) by excluding diffusion terms $(\mu_n^\alpha T_n^\alpha + \mu_p^\alpha T_p^\alpha) \frac{\partial}{\partial x} \delta n_\alpha$. Flux F_{dr}^α defined as

$$\begin{aligned} F_{dr}^\alpha = & -(2\mu_n^\alpha + \mu_p^\alpha) \delta n_\alpha \frac{\partial \varphi}{\partial x} + \\ & 2 \frac{\partial}{\partial x} (\mu_n^\alpha T_n^\alpha) \delta n_\alpha - \frac{\partial}{\partial x} (\mu_p^\alpha T_p^\alpha) \delta n_\alpha \end{aligned} \quad (27)$$

Spatio-temporal distribution of excess carrier concentrations

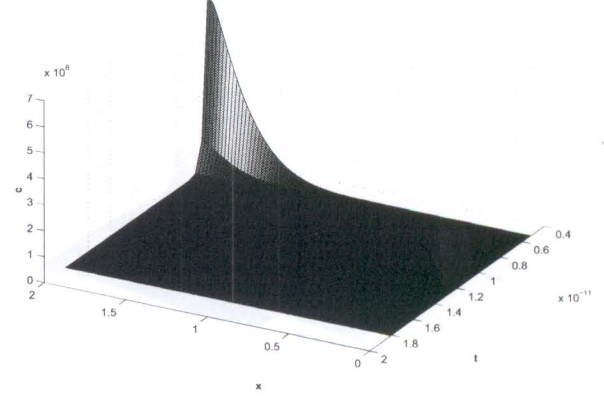


Fig. 8. Diffusion processes in the VFEPT structure

is also drift dominated, and is obtainable from (11) in a way similar to F_d^α , with additional exclusions of diffusive terms $\mu_n^\alpha T_n^\alpha \frac{\partial p_\alpha}{\partial x} - \mu_p^\alpha T_p^\alpha \frac{\partial n_\alpha}{\partial x}$ and replacing values n_α and p_α by δn_α . By analysing (25) we conclude that the difference scheme under consideration has the first order truncation error $\mathcal{O}(\delta^{-1}h)$ if $\Delta \rightarrow 0$. In those case where $\Delta \rightarrow \infty$ the scheme is also of the first order (for fluxes F_{dr}^α), but its truncation error can be represented as $\mathcal{O}(\Delta^2 h / ((\delta + \Delta)^2))$. Finally, note that according to (25) first order schemes may degrade in those cases where $\delta \rightarrow 0$. In the next section we apply the scheme discussed in this section to the analysis of VFEPT structures, concentrating on the case of $\Delta \rightarrow \infty$. All computational experiments reported below have been obtained under the assumptions $\mu_p^\alpha = \mu_n^\alpha = \text{const}$ and $p_\alpha \rightarrow 0$ in the domain of interest.

V. COMPUTATIONAL ANALYSIS OF CHARGE TRANSPORT PROCESSES IN VFEPT STRUCTURES

Our case study example is based on the analysis of charge photoresponse in the base of a GaAs vertical field-effect phototransistor structure. The schematic cross section of the structure is given in Fig.1. The gate (denoted by “g”) is $2 \mu\text{m}$ long and is located in the structure at equal distance $2 \mu\text{m}$ from the source (denoted by “s”) and drain (denoted by “d”).

Our first experiment demonstrates a “pure” drift phenomenon of concentrations in the case where at both ends of the structure Dirichlet boundary conditions are imposed. Figures 2 and 3 show the evolution of that drift along the structure. In this case the time of this drift for the $1 \mu\text{m}$ structure is estimated theoretically as $t_{dr} = (\mu_n^\alpha |\partial \varphi / \partial x|)^{-1}$, and for values $\mu_n^\alpha = 7000 \text{cm}^2 \text{V}^{-1} \text{s}^{-1}$ and $\partial \varphi / \partial x = 10^6 \text{Vcm}^{-1}$, used in our calculation, $t_{dr} = 1.4 \times 10^{-12} \text{s}$, which is in a good agreement with numerical results.

A more complicated situation arises where the reported phenomena may also be supplemented by some diffusion processes. In the remaining part, we consider the photocharge response in the depletion region of the structure

(between gate and drain). In this region conductive carries concentration is fairly low, and we assume that $n_c = p_c = 0$. Exceeded hole concentration is assumed to be $p_e = p_{e0} = 1\text{cm}^{-3}$. In this case we are interested in the behaviour of exceeded electrons with concentration n_e which propagate towards drain in the x -direction, as depicted in Fig. 1. Drain region is positively biased with 2 V potential. This voltage is applied to the region of $2\text{ }\mu\text{m}$, from the origin $x = 0$ to $x = L$. The boundary conditions for concentration $n_e = \delta n_e + p_{e0}$ were chosen in the Dirichlet form at $x = 0$ and in the Neumann form at $x = L$. In particular, results of computations reported here were obtained for the following boundary conditions

$$\begin{aligned}\delta n_e(x, t) &= n_0/10^{12} - p_{e0}, \quad x = 0; \\ \frac{\partial}{\partial x}(\delta n_e(x, t)) &= 0, \quad x = L.\end{aligned}\quad (28)$$

In (28) n_0 is GaAs intrinsic concentration at given temperature T_0 which was taken in our calculations as 320 K . Photo charge propagation was analysed with a coupled system of equations discussed in the previous sections

$$\frac{\partial \delta n_e}{\partial t} - \frac{\partial}{\partial x} F^e = G(x, t), \quad \frac{\partial}{\partial x} \left(\kappa \frac{\partial \varphi}{\partial x} \right) = \delta n_e. \quad (29)$$

Photogenerated carrier source was defined as $G(x, t) = G_0 \sin(\pi t/t_g)$ for $x \in [x_l, x_r]$ with $x_l = 0.85\text{ }\mu\text{m}$, $x_r = 1.15\text{ }\mu\text{m}$ and for $t \leq t_g = 10^{-19}\text{ s}$. We took $G_0 = 10^{32}\text{ cm}^{-3}\text{ s}^{-1}$. Otherwise, for $x \leq x_l$, $x \geq x_r$, $t \geq t_g$, $G(x, t) = 0$. The flux F^e was defined by equation (11) with mobility $\mu_n^e = 8000(300/T_0)^{2/3}\text{ cm}^2\text{ V}^{-1}\text{ s}^{-1}$.

The system of equations (29) was solved by using the scheme described in the previous sections. The actual implementation of the scheme was carried out in a semi-implicit manner

$$\left(\Lambda \left((\beta_n^e)^* \right)^k \delta n_e^{k+1} \right)_i = -\frac{(\delta n_e)_i^l}{\tau_{l+1}}, \quad (30)$$

$$\begin{aligned}\left(\Delta^h(\varphi)^{k+1} \right)_i &= \delta n_e^{k+1} + \\ (n_e^{k+1} + p_{e0})\alpha_{i+1/2} &(\varphi_i^{k+1} - \varphi_i^k),\end{aligned}\quad (31)$$

where $\Delta^h(\varphi) = (\varphi_{i+1} - 2\varphi_i + \varphi_{i-1})$ is the central difference operator, and k is the iteration number. The absolute stability of the scheme can be shown in a way similar to that developed originally in [7]. Iterative parameters $\alpha_{i+1/2}$ were chosen as follows (e.g., [7]):

$$\alpha_{i+1/2} = \frac{(\mu_n^e)_{i+1/2} \gamma_{i+1/2} \tau_{l+1}}{1 + (\mu_n^e)_{i+1/2} \gamma_{i+1/2} \tau_{l+1}}, \quad (32)$$

with $\gamma_{i+1/2} = 4/h_i^* (1/h_{i+1} + 1/h_i)$.

In Figures 4 and 5 we present the spatio-temporal distribution of the potential energy. It can be seen that after the photogeneration process (after approximately $1. \times 10^{-19}\text{ s}$) the potential energy raises and reaches its maximal value

in the middle of the structure. Then, up to the time moment estimated approximately as $1. \times 10^{-12}\text{ s}$ electrons tend to propagate from the maximal values of potential energy to boundary, where the potential energy is lower. In this case we clearly see that the concentrations achieve the same value at all spatial points of the structure. After the relaxation processes (presented in Fig. 6 and 7), drift-diffusion processes become essential (due to the imposed Dirichlet boundary condition, see Fig. 8). Theoretically estimated diffusion time of these processes $t_{\text{dif}} = L^2/4D$ with diffusion coefficient $D = k_B T_0 / q \mu_n^e$ and $L = 2\text{ }\mu\text{m}$ is in a good agreement with the results of computations.

VI. CONCLUSIONS

In this paper a model for the description of fast charge processes in optically sensitive semiconductors was derived and analysed numerically. For the solution of the problem we proposed an unconditionally monotone scheme. Computational analysis of a VFEPT was carried out for different situations and theoretical estimates of photo response (i.e. the time needed to achieve the steady state) were compared with the results of numerical calculations.

REFERENCES

- [1] S.A. Abashkina, V.I. Korol'kov, J.S. Rimshans, Y.I. Skryl', T.S. Tabarov, "Numerical Calculations of Transient Characteristics of GaAs Vertical Field-Effect Phototransistors", *Semiconductors*, Vol. 27(6), pp.524-529, 1993.
- [2] D.-F. Guo, "Optoelectronic switch performance in double heterostructure-emitter bipolar transistor", *Solid-State Electronics*, Vol. 45, pp.1179-1182, 2001.
- [3] N.V. Karetkina, "An unconditionally stable difference scheme for parabolic equations with first derivatives", *Computational Math. and Math. Physics*, Vol. 20(1), pp.236-240, 1980.
- [4] M. Kunst, F. Wunsch, and S. von Aichberger, "Recombination at high charge carrier concentrations in a Si:H films", *Thin Solid Films*, Vol. 383, pp.274-276, 2001.
- [5] R.V.N. Melnik and H. He, "Modelling nonlocal processes in semiconductor devices with exponential difference schemes", *J. of Engineering Mathematics*, Vol. 38, pp.233-263, 2000.
- [6] R.V.N. Melnik, "The alternating-triangular algorithm for the analysis of blow-up and quenching phenomena in nonlinear PDEs", *Mathematical Algorithms*, Vol. 2, pp.89-120, 2000.
- [7] B.S. Polsky and J.S. Rimshans, "Half-implicit difference scheme for numerical simulation of transient processes in semiconductor devices", *Solid State Electron.*, Vol. 29, pp.321-324, 1986.
- [8] V. Ryzhii, I. Khmyrova and M. Shur, "Terahertz photomixing in QW structures using resonant excitation of plasma oscillations", *J. of Applied Physics*, Vol. 91(4), pp.1875-1881, 2002.
- [9] A.A. Samarskii, *The theory of difference schemes*, Marcel Dekker, N.Y., 2001.
- [10] A.J. Shields et al, "Optically induced bistability in the mobility of a 2D electron gas coupled to a layer of quantum dots", *Appl. Phys. Lett.*, Vol. 74(5), pp.735-737, 1999.
- [11] F. Qian et al, "Indirect-coupling UV-sensitive photodetector with high electrical gain, fast response, and low noise", *Sensors and Actuators*, Vol. 86, pp.66-72, 2000.

CONTENTS

1. An Intelligent Control Using Variable Structure for Robot Manipulators(1)
Jing He, Changfan Zhang, Yonghong Long	
2. An Application of Universal Learning Networks in the Speed Control of DC Motor Drives Fed from a Photovoltaic Generator(5)
Ahmed Hussein, Kotaro Hirasawa, Jinglu Hu	
3. On the Boundedness Nature of Positive Solutions of the Difference Equation $x_{n+1} = \max(A_n/x_n, B_n/x_{n-1})$ with Periodic Parameters(11)
C.M. Kent, M.A. Radin	
4. Fast Computation of Derivatives in Control - An Approach based on Automatic Differentiation(16)
Klaus Röbenack	
5. Estimation of Time Delays in Multirate Sampled-Data Systems(23)
Jie Sheng, Tongwen Chen, Sirish L. Shah	
6. A convergence result for digital implementation via the bilinear and step-invariant transformations(28)
Guofeng Zhang, Tongwen Chen	
7. Asymptotic Expansions of Solutions of Cross-Coupled Algebraic Riccati Equations of Multimodeling Systems Related to Nash Games(34)
Hiroaki Mukaidani, Tetsu Shimomura, Hua Xu	
8. An LMI Approach to Guaranteed Cost Control of Nonlinear Large-Scale Uncertain Delay Systems under Controller Gain Perturbations(40)
Hiroaki Mukaidani, Yoshiyuki Tanaka, Hua Xu	
9. An Advanced Island Based GA For Optimization Problems(46)
H. Homayounfar, S. Areibi, F. Wang	
10. Inverse Dynamics Terminal Sliding Mode Control of Two-link Flexible Manipulators(52)
Yong Feng, Sheng Bao, Jiang Chengguo, Xinghuo Yu	
11. Reliable Control of Uncertain Delayed Systems with Integral Quadratic Constraints(58)
Chuwang Cheng, Qing Zhao	
12. Integrated Diagnosis and Reconfigurable Control for Actuator and Sensor Faults in a Pressurizer of a Nuclear Plants(64)
Jin Jiang, Youmin Zhang	
13. Modular Arithmetic and Synchronized Chaos(70)
William F. Langford, Steven Sladewski	
14. Analysis of controllability and observability of linear system	

To Index

with structured uncertainties Using monotonization methods	(76)
Takeshi Kawamura, Masasuke Shima	
15. Numerical Computation of Bifurcation in a Simple Baroclinic Flow	(82)
Gregory M. Lewis, Wayne Nagata	
16. On the Existence of Periodic Solutions of a Forced Duffing Equation	(88)
Chunqing Lu	
17. Solutions of a Pair of Conservation Laws with Nonconvex Flux Function	(92)
Sadao Shimoji	
18. A Novel Sensor-based Motion Planning Algorithm for Mobile Robots in Unknown Environments	(96)
Ming Lin, Jihong Zhu, Zengqi Sun	
19. Numerical Analysis of Fast Charge Transport in Optically Sensitive Semiconductors	(102)
Roderick V.N. Melnik, Janis Rimshans	
20. Real Solution Structure Analysis of the Direct Kinematics for a Parallel Manipulator	(108)
Qizhi Wang, Zhuqing Wang	
21. Numerical Approximation of the Solution for the Reaction-Diffusion System Modeling the Interaction of Two Predators and One Prey	(112)
Luis Fernando Hernández Moguel, Eric J. Avila Vales, A. Estrella González, M. Escalante Torres	
22. A Piecewise-linear Map for Finding Edges in Images	(117)
W. Yao, R.E. Ellis	
23. Computation of the Normal Form for 1:1 Resonant Double Hopf Bifurcation	(121)
Pei Yu	
24. The Simplest Normal Form of Generalized Hopf Bifurcation with Perturbation Parameters	(127)
Pei Yu, Yuan Yuan	
25. An Approach to Adaptive Multimodal Biometric Fusion	(133)
Qinghan Xiao	
26. Classification Using Feature Interval Selection	(137)
David K.Y. Chiu, Bogdan J. Buczynski	
27. Practical Tuning of Two-Input Two-Output Takagi-Sugeno Fuzzy Controllers with Simplified Rule Consequent	(142)
A. Alwadie, H. Ying, and H. Shah	
28. A Prony Approach to Modeling of Time-Varying Fuzzy Systems	(147)
Trung T. Pham, Guanrong Chen	
29. Global Dynamic Optimization of Linear Time Varying Hybrid Systems	(153)

MR2015793 82D37

Melnik, Roderick V. N. [[Melnik, Roderick V. Nicholas](#)] (DK-SU-IPI);
Rimshans, Janis (LA-LATV-CS)

**Numerical analysis of fast charge transport in optically sensitive
semiconductors. (English summary)**

Engineering applications and computational algorithms (Guelph, ON, 2003).

Dyn. Contin. Discrete Impuls. Syst. Ser. B Appl. Algorithms **2003**, suppl., 102–107.

© Copyright American Mathematical Society 2021